

1965

Design and Testing of Experimental Components Used on Photoelastic Analysis

Alan Rae Peterson

Follow this and additional works at: <https://openprairie.sdstate.edu/etd>

Recommended Citation

Peterson, Alan Rae, "Design and Testing of Experimental Components Used on Photoelastic Analysis" (1965). *Electronic Theses and Dissertations*. 3069.
<https://openprairie.sdstate.edu/etd/3069>

This Thesis - Open Access is brought to you for free and open access by Open PRAIRIE: Open Public Research Access Institutional Repository and Information Exchange. It has been accepted for inclusion in Electronic Theses and Dissertations by an authorized administrator of Open PRAIRIE: Open Public Research Access Institutional Repository and Information Exchange. For more information, please contact michael.biondo@sdstate.edu.

14

DESIGN AND TESTING OF EXPERIMENTAL COMPONENTS USED
IN PHOTOELASTIC ANALYSIS

BY

ALAN RAE PETERSON

A thesis submitted
in partial fulfillment of the requirements for the
degree Master of Science, Major in
Mechanical Engineering, South
Dakota State University

1965

**DESIGN AND TESTING OF EXPERIMENTAL COMPONENTS USED
IN PHOTOELASTIC ANALYSIS**

This thesis is approved as a creditable and independent investigation by a candidate for the degree, Master of Science, and is acceptable as meeting the thesis requirements for this degree, but without implying that the conclusions reached by the candidate are necessarily the conclusions of the major department.

Thesis Adviser

Date

**Head, Mechanical
Engineering Department**

Date

30.1A

ACKNOWLEDGMENTS

To Mr. Lloyd D. Lee, Assistant Professor, Department of Mechanical Engineering, the author wishes to extend sincere appreciation for his assistance and cooperation in writing this research report.

This thesis is dedicated to my wife, Janice, for her loyal support and encouragement throughout the course of the Master of Science program.

ARP

TABLE OF CONTENTS

	Page
CHAPTER I. INTRODUCTION	1
CHAPTER II. THEORY OF PHOTOELASTICITY	3
A. History	3
B. Field of Application.	4
C. Electromagnetic Theory of Light	6
D. Stresses within a Body.	12
E. Application of Light Theory to Photoelastic Stress Analysis	14
CHAPTER III. EXPERIMENTAL APPARATUS	22
A. Polariscopes	22
B. The Stress-Freezing Oven.	24
C. The Loading Frames.	26
D. Model Cutter.	29
CHAPTER IV. LABORATORY TEST PROCEDURE	31
A. Photoelastic Material and Equipment Arrangement .	31
B. Fringe Calibration at Normal Temperature.	33
C. Fringe Calibration at Elevated Temperature.	39

	Page
D. Determination of the Stress-Trajectories	42
CHAPTER V. CONCLUSIONS AND RECOMMENDATIONS	44
BIBLIOGRAPHY.	46
APPENDIX A.	47
APPENDIX B.	51
APPENDIX C.	55
APPENDIX D.	57

LIST OF FIGURES

Figure		Page
I.	Light Function.	7
II.	Ordinary Light Vector	8
III.	Plane Polarization.	9
IV.	Doubly Refracted Light Ray.	11
V.	Positive Stress Directions.	12
VI.	Direction of Vibration of a Polarized Ray OU. . . .	16
VII.	The Chapman Technical Polariscopes	23
VIII.	The Stress-Freezing Oven Showing Heating Units, Loading Frame and Firebrick for Heat Storage. . . .	25
IX.	Tension and Compression Loading Frame with Attaching Fixtures.	27
X.	Frame for Bonding Moment.	27
XI.	Ratio of Moment to Tension.	28
XII.	Precise Photoelastic Model Cutter	30
XIII.	Specimen before Annealing.	32
XIV.	Specimen after Annealing.	32
XV.	Sequential Photograph Showing Linear Stress- Optic Relationship	34
XVI.	Standard Tension Specimen	36
XVII.	Diametrically Loaded Circular Disk.	38
XVIII.	Frozen-Stress Pattern	41
XIX.	Picture Showing Undisturbed Fringes in Frozen Model.	42

Figure	Page
XX. Construction of Lines of Principal Stress	42
XXI. Isoclinic Fringes in Compressed Disk.	49
XXII. Stress Trajectories in Compressed Disk.	49
XXIII. Relative Retardation in Compressed Disk Shown in Figure XVII.	50
XXIV. Curved Beam Specimen.	52
XXV. Isoclinics in Curved Beam Specimen.	53
XXVI. Sketch of Stress Trajectories in a Curved Beam. . .	54
XXVII. Cooling Curves for Stress-Freezing Oven	56

LIST OF TABLES

Table		Page
1.	Fringe Ratio Under Varying Loads	33
2.	Tabular Form for P and Q Values on Circular Disk	48

CHAPTER I

INTRODUCTION

Exact solutions of the stress distribution in elastic bodies are confined to a select group of geometric configurations. The nature of irregular-shape problems prohibits a solution by closed formula or even by a general form of solution. A numerical or experimental approach is then dictated. Strain gauges, stress coatings, and photoelastic methods are all tools used for the experimental analysis of irregular shapes.

All experimental techniques have weaknesses which limit their usage. Strain gauges give a numerical solution but only at a surface. Actual loading conditions in a partial model are seldom possible; therefore, strain gauges cannot be effectively applied to cross-sectional studies.

Stress coatings are materials which will fail when a prescribed stress value is reached. Such brittle coatings will show the direction, magnitude, and distribution of tensile stresses over an entire surface but they are restricted to some designated level of failure.

Two-dimensional photoelastic studies require a model of the prototype and a polariscope. The model is a photoelastic specimen dimensionally similar to the prototype. Although the method of

interpretation is more involved than the study of stresses by strain gauges or stress coatings, a photoelastic analysis will give a more complete stress picture in the model as well as the principal stress values. Photoelasticity is an experimental technique which will effectively measure the stresses in a cross-sectional area. Many stress problems which are either too time consuming or are impossible to solve by mathematical models lend themselves readily to a photoelastic study.

Irregularities such as connectors, holes, notches, and other shape complexities cause stress concentrations which are impossible to evaluate. Actual machine parts which have stress-concentrations in three-dimensions can be analyzed by three-dimensional photoelastic methods. A model is made, loaded, heated to the critical temperature of the plastic, and cooled at a controlled rate. This procedure freezes the stresses into the model so that any plane may be removed and analyzed.

Severe changes in the stress-optic constants and mechanical properties of photoelastic material are observed at the critical temperatures of stress-freezing. This thesis will be concerned with the establishment of a fundamental laboratory procedure and the calibration of the equipment for a complete photoelastic analysis.

CHAPTER II

THEORY OF PHOTOELASTICITY

A. History

Observations of colored patterns in stressed glass when examined in polarized light were first made by Brewster in 1816.^{1/} Neuman, Maxwell, Wertheim, and other noted physicists developed the theory that the patterns were of optical retardation resulting from a change in density. The optical retardation of light is proportional to the principal stresses in the glass.^{2/} Not until the beginning of the twentieth century were these fundamental principles applied to engineering techniques. A Treatise on Photoelasticity published in 1931 by Coker and Filon was the first publication to present a systematic procedure for stress analysis by photoelastic methods.

Although World War II interrupted the development of the photoelastic method of stress analysis, two important by-products of wartime technology were of great value. New plastic resins and a polaroid lens which would economically project large beams of polarized light made widespread usage possible. More economical tools for study led to rapid advancement of the science.

^{1/} Dove, Richard C. and Paul H. Adams, Experimental Stress Analysis and Motion Measurement. Columbus: Charles E. Merrill Books, Inc., 1964, p. 288.

^{2/} Hetenyi, M., Handbook of Experimental Stress Analysis. New York: John Wiley and Sons, Inc., 1950, 829.

B. Field of Application

Photoelastic methods form a direct link between mathematical analysis and irregular shapes. Photoelasticity may also be used as a supplementary tool to general formulas to calculate concentration factors.

There are several advantages and disadvantages of these methods over alternative methods of stress analysis because it is an experimental technique. Some of the main advantages^{3/} of the photoelastic methods of stress analysis are that they provide a means of:

1. Obtaining an over-all picture of the shearing stress distribution.
2. Measurement of stress at a point with consequent possibility of finding actual peak values even in regions of high stress gradient.
3. Determination of stresses in two-dimensional problems that cannot be solved analytically.
4. Accurate stress determination in irregular members comparable to results obtained with precise strain-gauge techniques.
5. Readily obtaining qualitative results for location of minimum - and maximum - stress locations or for the determination of changes in stress distribution caused by minor alterations in shape of the model to aid in the process of developing a satisfactory design.

The shortcomings of this experimental technique and some of the disadvantages appear to be as follows:

^{3/}Ibid., p. 832.

1. It is an indirect method requiring the use of accurate scale models and subsequent interpretation of data for the prototype.
2. The experimental procedure is readily applied only to two-dimensional conditions, since the three-dimensional methods require rather involved and carefully developed techniques.
3. The separation of the individual principal stresses at interior points in the model becomes rather troublesome if great accuracy is required.
4. For proper application a carefully developed experimental procedure must be followed including the necessity of preparing models that are stress-free.
5. The applications of the method are limited to the determination of elastic stresses due to externally applied forces. The method will not yield information relative to the influences of surface conditions on the prototype (such as microscopic corrosion pits and machining scratches) nor can it be used to determine the residual stresses or the elastic redistribution of stress that occurs after the prototype has undergone some plastic deformation, heat treatment, or welding operation.

Statement one of the shortcomings of photoelastic analysis could be modified to include the fact that a different material is being used to make the model of the prototype. Known photoelastic materials do not always behave proportionally to the prototype material with respect to all mechanical properties. Statement two of the shortcomings explains that the three-dimensional photoelastic methods are difficult, but it does not mention that these are the only methods of cross-sectional analysis presently available.

C. Electromagnetic Theory of Light

Photoelastic methods of stress analysis are dependent upon the behavior of light. Light is thought to be an electromagnetic disturbance consisting of transverse waves propagated along straight lines. The wave is composed of two effects mutually perpendicular at any point in space. One effect is electric and the other is magnetic; each effect can be represented by a vector at any given time. The electric vector is considered to be the light vector.

Although white light contains all of the different frequencies of vibration of the visible spectrum ($f = 390 \times 10^{12}$ to 770×10^{12} cps.), monochromatic light, the homogeneous light used in photoelastic studies, is a light having only one frequency of vibration.

An isolated light wave may be described as having a frequency of vibration f , a wavelength λ , and a velocity c . These are related by the expression

$$\lambda \cdot f = c = 3 \times 10^{10} \text{ cm/sec.} \quad \text{Eq. (1)}$$

Mathematical representation^{4/} of a light wave at any time is

$$U = a \sin \frac{2\pi}{\lambda} (v_0 t - x + e). \quad \text{Eq. (2)}$$

^{4/}Ibid., p. 836.

This relation of a light wave describes the graphical model shown in Figure 1.

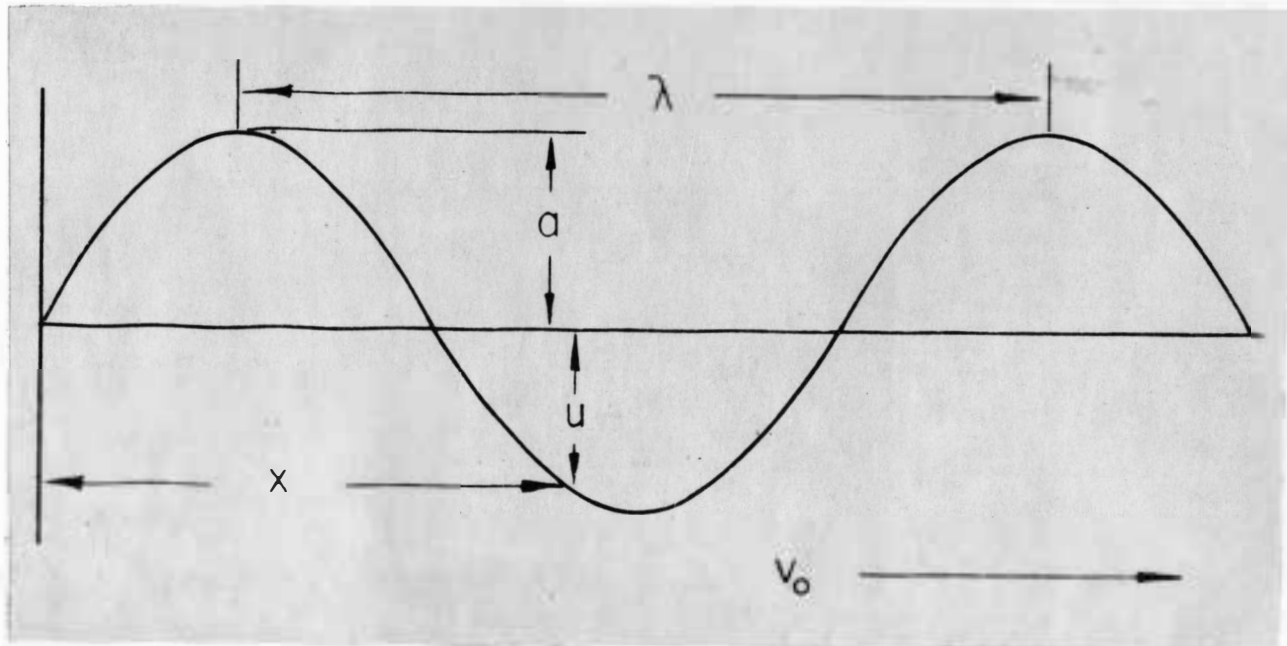


Figure 1. Light Function

where,

U = magnitude of the displacement given by the vector

a = amplitude

x = distance along light ray from some reference point

v_0 = velocity of propagation of light

t = time

e = a constant

Polarization is an act or process of controlling light in such a manner that its vectors assume a definite form or pattern. White light contains waves oriented into every conceivable position, Figure II.

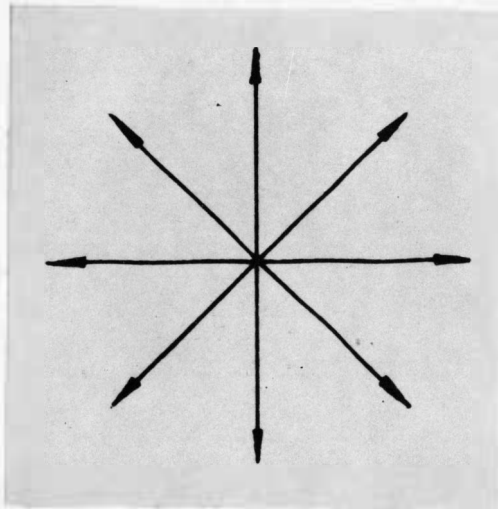


Figure II. Ordinary Light Vector

Upon polarization, only the vectors oriented in one particular direction will be transmitted. Waves oriented in this direction are in the plane of vibration. Perpendicular to the plane of vibration is the plane of polarization from which all light vectors have been removed, Figure III.

Three types of polarization exist: plane, elliptical, and circular polarization. Plane polarization has all vectors in one plane along the direction of propagation. Elliptical polarization exists when light is transmitted through a lens with the vectors

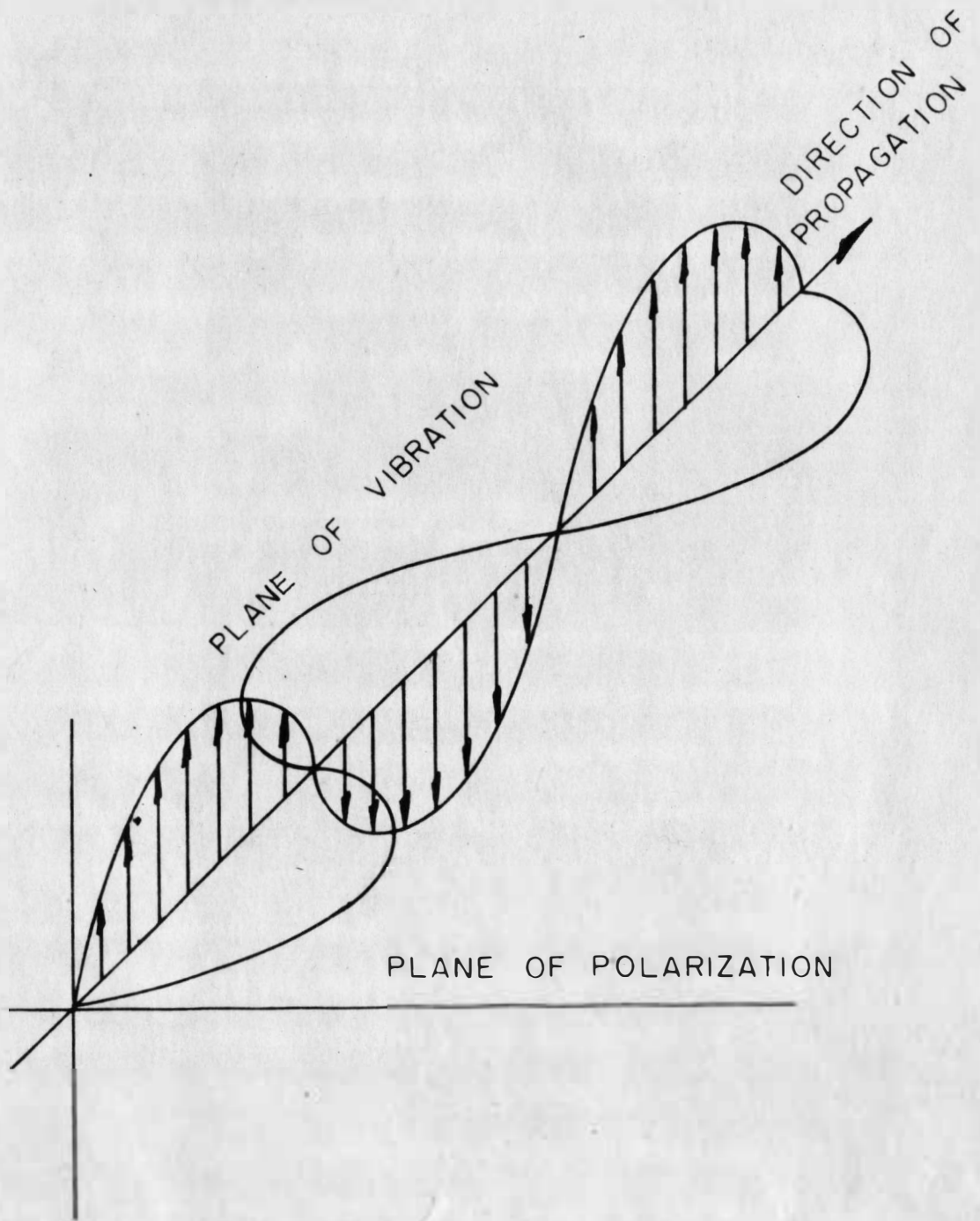


Figure III. Plane Polarization.

rotating around the line of propagation. The length of the vectors varies in a distinct period which forms an elliptical helix. Circular polarization is a special case of elliptical polarization; all vectors are constant length and form a circular helix.

Light velocity is changed in passing from one medium to another. The ratio of velocities in two different materials, is represented by the formula

$$N = \frac{\text{velocity in first material}}{\text{velocity in second material}}, \quad \text{Eq. (3)}$$

where N is the index of refraction.^{5/} Certain double refractive materials have different indices of refraction in different planes of the same specimen. Light which has passed through a double refractive material is broken into the linearly polarized rays, A and B, Figure IV.

Double-refractive crystals can be cut so that their faces are parallel to the optic axis and so that the two wave fronts are tangent to each other. Although the waves will not be separated, they will be out of phase with each other.

By using a proper combination of type of light and lens thickness, one may obtain light which is a quarter of a wavelength

^{5/} Richards, J. A., F. W. Sears, M. R. Wehr and M. W. Zemansky, Modern University Physics. Reading, Mass.: Addison-Wesley Publishing Company, Inc., 1960, p. 696.

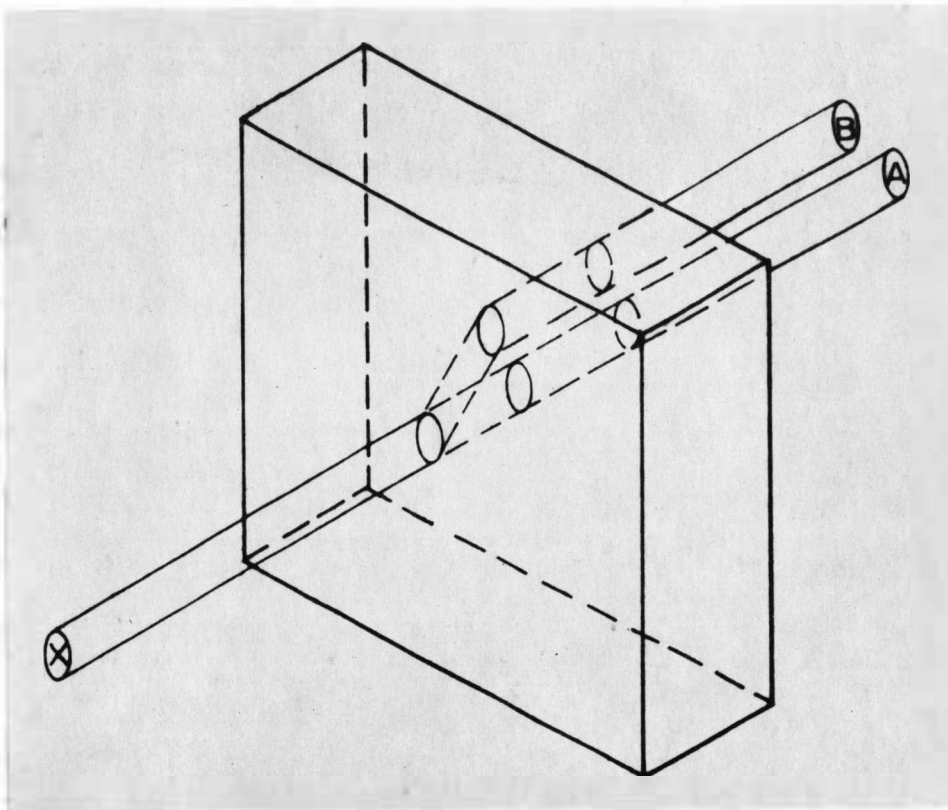


Figure IV.^{6/} Doubly Refracted Light Ray

out of phase with the original ray, resulting in circular polarized light.^{7/} When a model is examined in circular polarized light and then in plane polarized light, a complete photoelastic solution containing the shear stress, principal stress, and directions can be determined for any point on the model.

^{6/}Ibid., p. 698.

^{7/}Hetenyi, p. 837.

D. Stresses within a Body

Members loaded externally have a resulting internal reaction between molecules. A force in tension will cause the maximum normal stress in the plane perpendicular to the direction that the force is acting. The vertical shear stress will equal zero. On any plane other than one normal to the line of force, the shear and normal stresses form a polygon which is in equilibrium. Derived relationships for stresses assume that the body is perfectly elastic, homogeneous, and isotropic. Standard directional relationships for positive stresses are shown in Figure V.

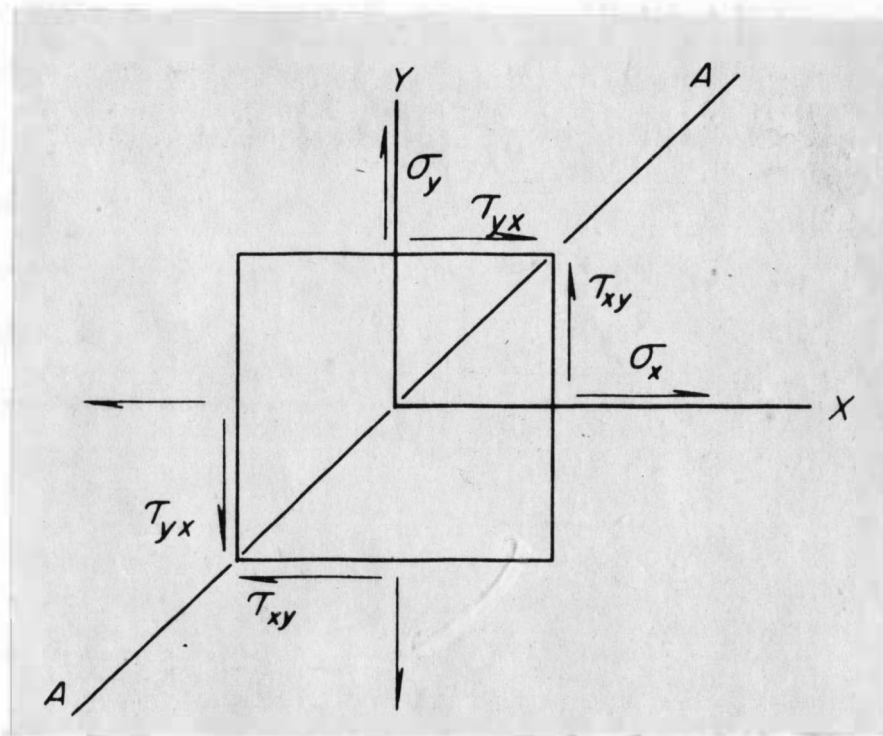


Figure V. Positive Stress Directions

The normal stresses σ_x and σ_y will be positive in tension.

Shearing stresses will be positive when the shear diagonal, A-A, passes through the first quadrant. For all types of loads, a shear stress at any point on one plane is accompanied by a shear stress of equal magnitude on an orthogonal plane through that point.^{8/}

Principal stresses, the maximum normal stress σ_1 , and the minimum normal stress σ_2 , in a stressed body occur on the principal plane. Principal normal stresses in a body can readily be found from Mohr's circle^{9/} to be:

$$\sigma_{1,2} = \frac{\sigma_x + \sigma_y}{2} \pm \sqrt{\frac{\sigma_x - \sigma_y}{2} + \tau_{xy}^2} \quad \text{Eq. (4)}$$

at any angle of the principal plane θ_p . Mohr's circle is a method of plotting the normal stresses against the shear stresses at a point. The resulting circular distribution facilitates either an analytical or a graphical solution of the stresses on any two-dimensional plane through that point. The maximum shear stress at a point is equal to one-half the difference between the two principal stresses,

$$\tau_{\max} = \frac{\sigma_1 - \sigma_2}{2} \quad \text{Eq. (5)}$$

and it exists at an angle of 45 degrees to the principal plane.

^{8/} Higdon, A., E. H. Ohlsen and W. B. Stiles, Mechanics of Materials. New York: John Wiley and Sons, Inc., 1960, p. 24.

^{9/} Ibid., p. 33.

E. Application of Light Theory to Photoelastic Stress Analysis

Neumann and Maxwell conducted studies in artificial double refraction in stressed bodies. They formulated the following two laws^{10/} in terms of stress:

1. At any point in a stressed transparent solid the axis of polarization of light passing through the solid are parallel to the directions of the principal stresses in the plane of the wave-front at that point.
2. The difference of the velocities of the two oppositely polarized rays at the point is proportional to the difference of these two principal stresses, and is independent of the stresses perpendicular to the wave-front.

Thus, optical retardation in a body is proportional to the stresses, the thickness, and the optical coefficient of the material. For a double-refractive material:

$$r_1 = c_1 \sigma d$$

$$r_2 = c_2 \sigma d$$

where,

r_1 = retardation for refractive index one

c_1 = optical coefficient for plane one

r_2 = retardation for refractive index two

^{10/} Jessop, H. T. and F. C. Harris, Photoelasticity Principles and Methods. New York: Dover Publications, Inc., 1949, pp. 36-37.

c_2 = optical coefficient for plane two

d = model thickness

and

$$r = r_1 - r_2 = c_1 \sigma d - c_2 \sigma d$$

$$r = r_1 - r_2 = \sigma d (c_1 - c_2) \quad \text{Eq. (6)}$$

r = relative retardation.

In the case of the principal stresses in the body the two normal stresses, σ_1 and σ_2 , are mutually perpendicular. For materials having two perpendicular normal stresses the retardation will be proportional to the sum of the retardation caused by each stress:

$$r_1 = c_1 \sigma_1 d + c_2 \sigma_2 d$$

$$r_2 = c_2 \sigma_1 d + c_1 \sigma_2 d$$

$$r_1 - r_2 = (c_1 - c_2) (\sigma_1 - \sigma_2) d$$

$$r = C (\sigma_1 - \sigma_2) d \quad \text{Eq. (7)}$$

where,

r = relative retardation

C = relative stress - optic coefficient

d = model thickness.

The optical retardation produced in a stressed plate begins with normal incidence upon the plate. This beam is split into two oppositely polarized rays. Interference fringes will be produced by the analyzer, a second polaroid lens. The two polaroid lenses and a light source comprise a plane polariscope. The lenses are crossed if the polarizer and analyzer are aligned so that the vibrations pass perpendicularly from the polarizer to the analyzer. There must be some distortion in the model between crossed lenses for any light to pass.

Considering the vector in Eq. (2),

$$U = a \sin \frac{2\pi}{\lambda} (v_0 t - x + e)$$

looking in the direction of the light ray, let OP represent the direction of the vibration leaving the polarizer, Figure VI.

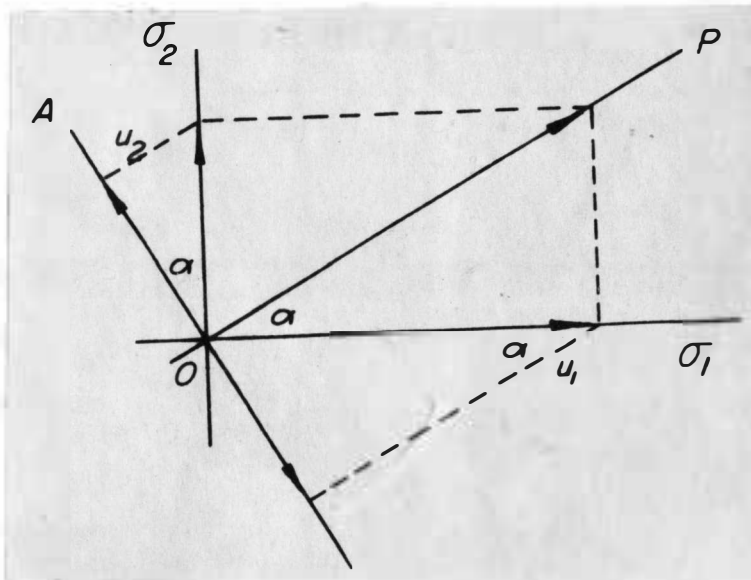


Figure VI. Direction of Vibration of a Polarized Ray OU.

Then consider some point O in the stressed model where the principal stresses σ_1 and σ_2 are α and $90^\circ - \alpha$, respectively from the plane of vibration, OP, of the light. The corresponding vectors^{11/}, $U_1 = U \cos \alpha$, and $U_2 = U \sin \alpha$, upon entering the model will be equal to

$$U_1 = a \cos \alpha \sin \frac{2\pi}{\lambda} (v_0 t - x) \quad \text{Eq. (8)}$$

$$U_2 = a \sin \alpha \sin \frac{2\pi}{\lambda} (v_0 t - x). \quad \text{Eq. (9)}$$

One wave will be retarded in the model by the amount r , Eq. (7)

$$r = C(\sigma_1 - \sigma_2) d.$$

These waves will then be:

$$U_1' = a \cos \alpha \sin \frac{2\pi}{\lambda} (v_0 t - x - r) \quad \text{Eq. (10)}$$

$$U_2' = a \sin \alpha \sin \frac{2\pi}{\lambda} (v_0 t - x) \quad \text{Eq. (11)}$$

From the model, the wave will enter the analyzer. The direction of the analyzer axis, OA, is perpendicular to the axis of the polarizer. The vectors on OA represent the light passing through the analyzer. The resultant light vector will equal the

^{11/} Ibid., pp. 65-66.

sum of the two components

$$U_1' \sin \alpha + (-U_2' \cos \alpha),$$

therefore,

$$a \sin \alpha \cos \alpha \left[\sin \frac{2\pi}{\lambda} (v_0 t - x) - \sin \frac{2\pi}{\lambda} (v_0 t - x - r) \right].$$

Writing the terms in the bracket as a product^{12/}, this becomes

$$U' = a \sin 2\alpha \sin \frac{\pi r}{\lambda} \cos \frac{2\pi}{\lambda} (v_0 t - x - r). \quad \text{Eq. (12)}$$

This light wave has the amplitude

$$A = a \sin 2\alpha \sin \frac{\pi r}{\lambda}. \quad \text{Eq. (13)}$$

The intensity of the emerging wave is equal to the amplitude squared. If in either condition $2\alpha = n\pi$ or $\frac{\pi r}{\lambda} = n\pi$, n equals either zero or an integer^{13/}, the intensity will equal zero. A maximum intensity exists when $2\alpha = 1$ or $\alpha = \frac{\pi}{4}$.

The light intensity will be zero when the principal stresses are parallel to the polarizer and analyzer respectively. A dark line will be projected from the model when the stresses are oriented

^{12/} Ibid., p. 66.

^{13/} Frocht, M. M., Photoelasticity, Vols. 1 and 2. New York: John Wiley and Sons, 1941, 1948, pp. 178-179.

parallel to the axis of the lenses. This is the case of $2\alpha =$ zero or n multiples of π . A locus of these points where the principal stresses have a constant direction forms an isoclinic line. By rotating the axis of the polarizer and analyzer, one may obtain isoclinic fringes which represent different principal stress orientations. Isoclinic lines actually appear as a diffuse fringe leaving the position of the true line to be judged by the eye.

Zero intensity also occurs at $r = n\lambda$, where r is the relative retardation equalling zero or some integral number of wavelengths. Since this is a relative retardation, the interference fringes from zero or an integral number of wavelengths of retardation will represent a stress difference. Light from a monochromatic light source will produce light and dark interference fringes in the stressed body. These lines of principal stress difference are isochromatic lines. If a white light source is used to view the model, the isochromatic lines will be a series of bands of brilliant colors. White light fails in regions of high stress because the different wavelengths will interfere with each other. White bands will be introduced causing a section where stresses cannot be interpreted.

A plane polariscope is sufficient for stress analysis, but it will project both isochromatic and isoclinic lines simultaneously. By mounting two quarter-waveplates on the polariscope, one between

the polarizer and the model and the second between the model and the analyzer, the plane polariscope is converted into a circular polariscope which will eliminate the isoclinic fringes without affecting the isochromatic lines. The quarter-waveplates are mounted in a "crossed" position at an angle of 45 degrees to the axis of the polarizer and analyzer. Light is extinguished in an isoclinic fringe. With the addition of the quarter-waveplates, the vibration is turned 45 degrees and passed through the polariscope. The condition of $\alpha = 0$ in Eq. (13) cannot occur in a circular polariscope; consequently the corresponding isoclinic fringes cannot occur.^{14/} The condition of $r = n\lambda$ is the same for both types of polariscopes so the isochromatic fringes remain intact.

Photoelastic solutions are taken from the combined use of the isochromatic and isoclinic patterns in a test specimen. Isoclinic lines are independent of the load because they are a result of stress direction, not magnitude. By rotating the polarizer and analyzer, the parameters of the isoclinic lines are made visible. This movement of the visible line means that the principal stresses vary from point to point. Isostatics or stress trajectories are taken from the traces of the isoclinics. A diagram of several of

^{14/}Ibid., p. 179.

these stress trajectories gives a good picture of the directions of the stress-distributions. Stress-trajectories are drawn mechanically from one isoclinic to another.

A second set of stress trajectories can be obtained by drawing a curve of normals to the original points of intersection. Principal stresses are mutually perpendicular; the mutually perpendicular stress trajectories represent the direction of the maximum and minimum normal stresses P and Q, respectively. The two isostatic lines obtained are the p and q lines, Figure XVII and Figure XVIII.

Isochromatic lines represent a stress difference by the relative retardation of light. Each material has a particular constant amount of retardation per level of stress difference. A tabular form is set up for the determination of the magnitude of each stress level, Appendix A.

CHAPTER III

EXPERIMENTAL APPARATUS

A. Polariscopes

The polariscopes are a Chapman 8-inch technical unit, Figure VII. It utilizes a straining frame with a dial indicator for two-dimensional analysis. Models up to 10 inches by 13 inches can be loaded on the frame in either tension or compression.

Light is supplied by a dual light source. One filament gives white light and the other is a low-pressure mercury arc. The mercury arc with a Wratten 77 filter isolates the 5460 Å monochromatic wave. Line voltage of 110 volts is the power source.

Laminated glass is used for the polarizer and analyzer lenses. They are mounted in a crossed relationship on a common drive mechanism. The mechanism is calibrated in five-degree increments.

The plane polariscopes are converted into a circular polariscopes by two quarter-waveplates. One is mounted between the polarizer and the straining frame, and the other between the straining frame and the analyzer. They are easily removed by removing two thumbscrews.

Data can be recorded either photographically or graphically with a special projector. The camera takes 4-inch by 5-inch film.

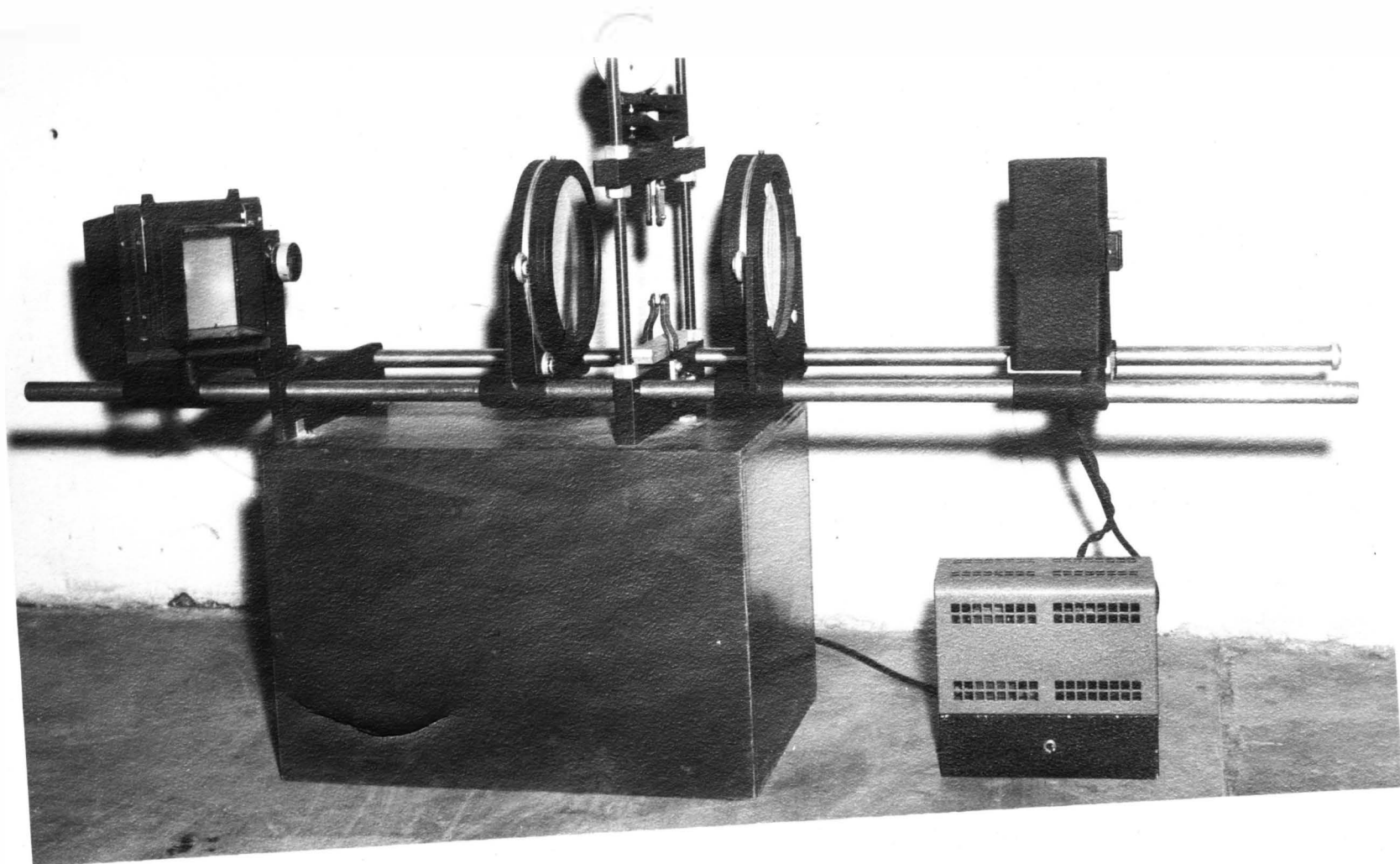


Figure VII. The Chapman Technical Polariscope.

A 9-inch maximum image is formed on the tabletop by the projection attachment. Spherical pyrex is used in the projector to minimize temperature distortion.

B. The Stress-Freezing Oven

A model can have stresses frozen into it by loading it, heating it and then cooling it at a controlled rate. From this model slices can be taken for analysis in various other planes. The stress-optic retardation in a stress-frozen specimen is proportional to the retardation observed at a normal temperature. If a slice is taken in a manner such that a minimum of heat is created, the stress-optic properties will remain intact through the cutting operation, Figure XIX.

The oven walls are 3.5 inches thick and are paneled with transite sheets. Insulation is provided by a packed zonolite filling. Four flat 1350 watt Type 56-KTS heating units are mounted on the inside oven walls. They are controlled by a model W-50, 120 volt Variac. Temperatures can be read by a mercury thermometer or by an iron-constantan thermocouple recording thermometer. The oven well is 35 inches by 29 inches by 22 inches. Enough space is available to permit a fire brick lining for its heat holding capacity.

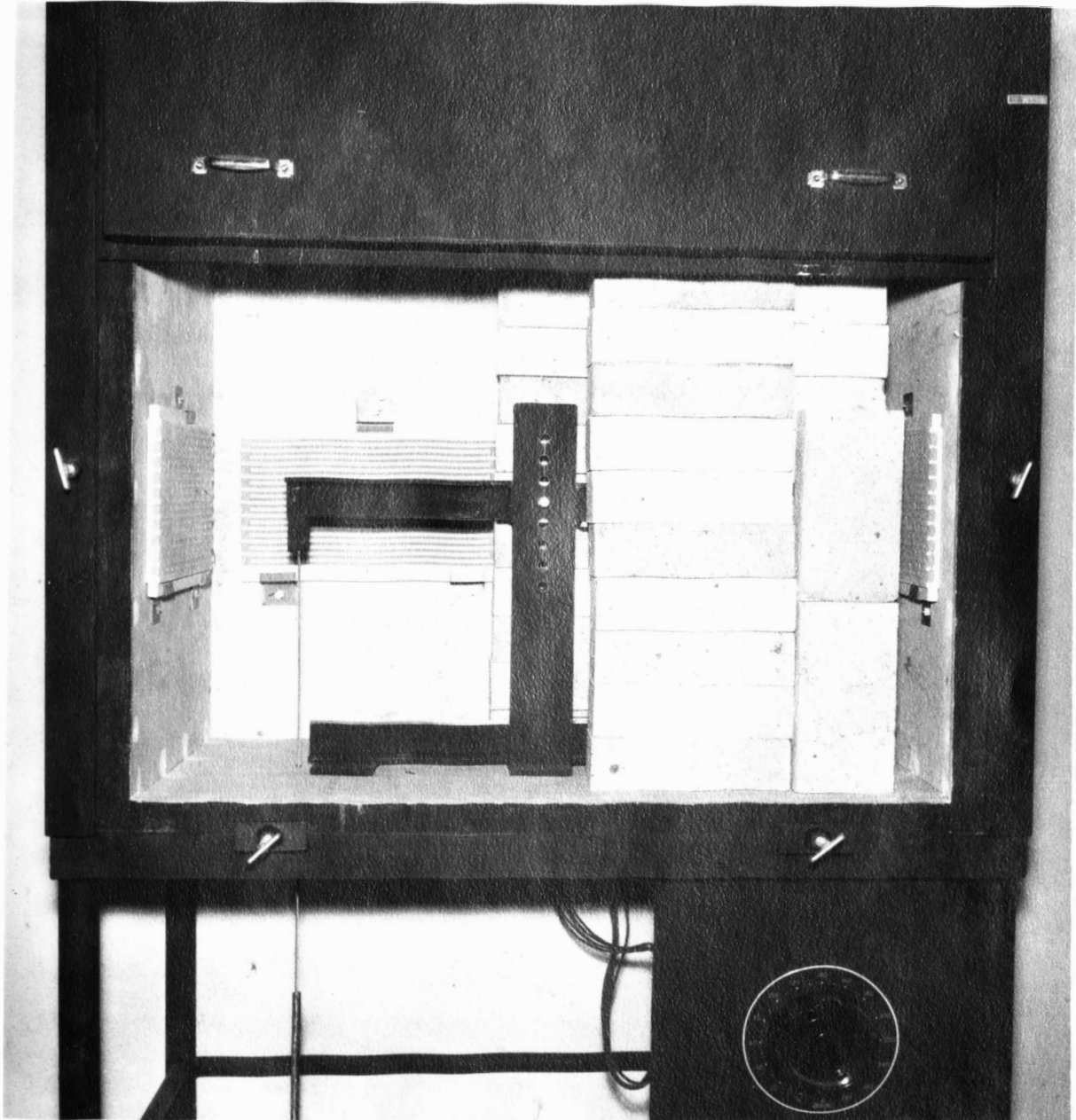


Figure VIII. The Stress-Freezing Oven Showing Heating Units, Loading Frame and Firebrick for Heat Storage.

C. Loading Frames

Particular purpose loading frames to handle general-sized models have been designed for this thesis. Loads under compression, tension, and a moment in either of two planes can be created inside of the oven.

One frame was designed to load a model in either tension or compression, Figure IX. It will handle test pieces varying from 1 to 9 inches. Friction has been minimized by placing two bearings, one on each side of the frame, at the balance points. All other connections are made with knife's edges to make the measurement more accurate.

The holding fixture shown is positioned by measuring to the vertical line on the support standard. Since the part is in tension, the model is placed loosely into the fixtures, loaded, and then tightened. This procedure insures perfect alignment of the line of force and minimizes the effects of an induced moment.

Moment effects can be even more pronounced in compression, and are more difficult to eliminate. The two fixtures shown in Figure IX are used in compression. Note the knife's edge on the bottom of each fixture. By stressing the model through a knife's edge, induced moments are eliminated. As the load is applied, the fringe pattern should be symmetrical to indicate that the load is being applied through the proper axis.

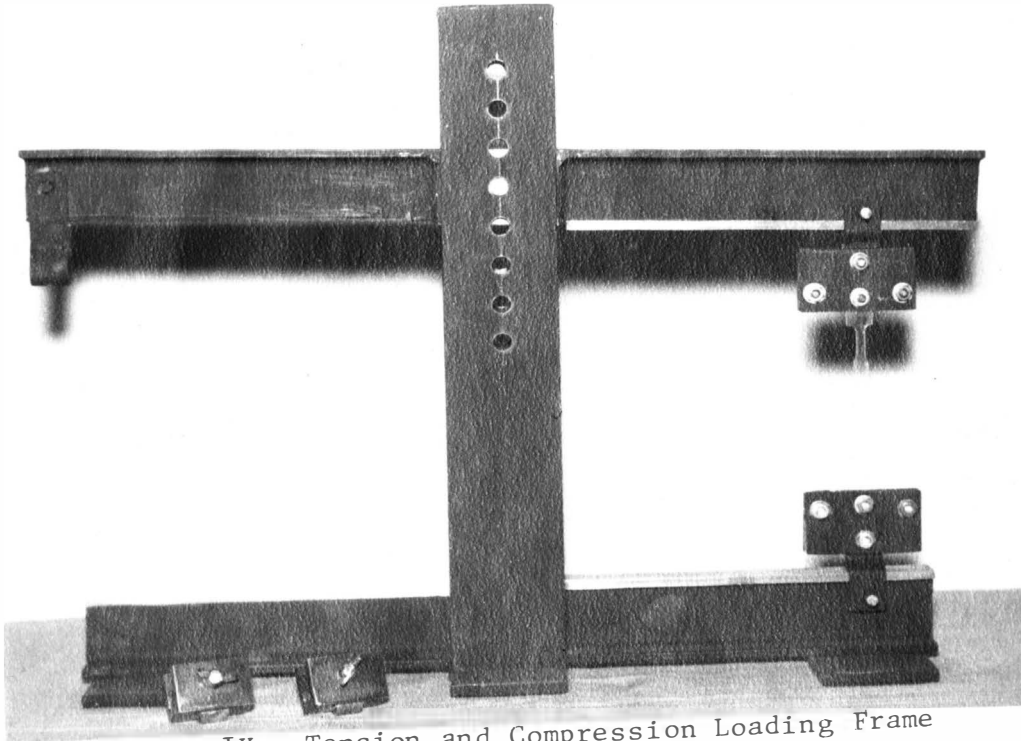


Figure IX. Tension and Compression Loading Frame with Attaching Fixtures.

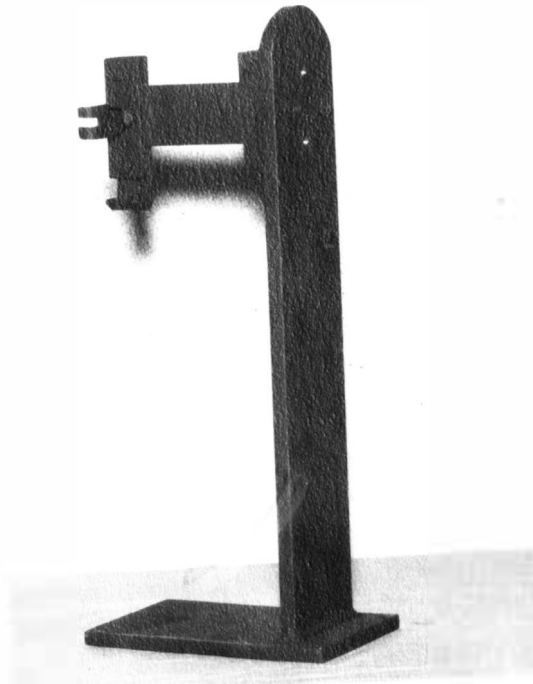


Figure X. Frame for Bending Moment.

Bending moment can be exerted on a model in the frame shown in Figure X. A combination of bending moment and tension can be obtained in most proportions by placing the model at selected angles. The angle desired can be determined trigonometrically by the ratio of tension, T, to moment, M, Eq. (14), Figure XI.

$$\theta = \text{Arctan} \frac{M}{T} \quad \text{Eq. (14)}$$

The load P is also determined trigonometrically to be

$$P = \frac{T}{\text{Cos} \theta} \quad \text{Eq. (15)}$$

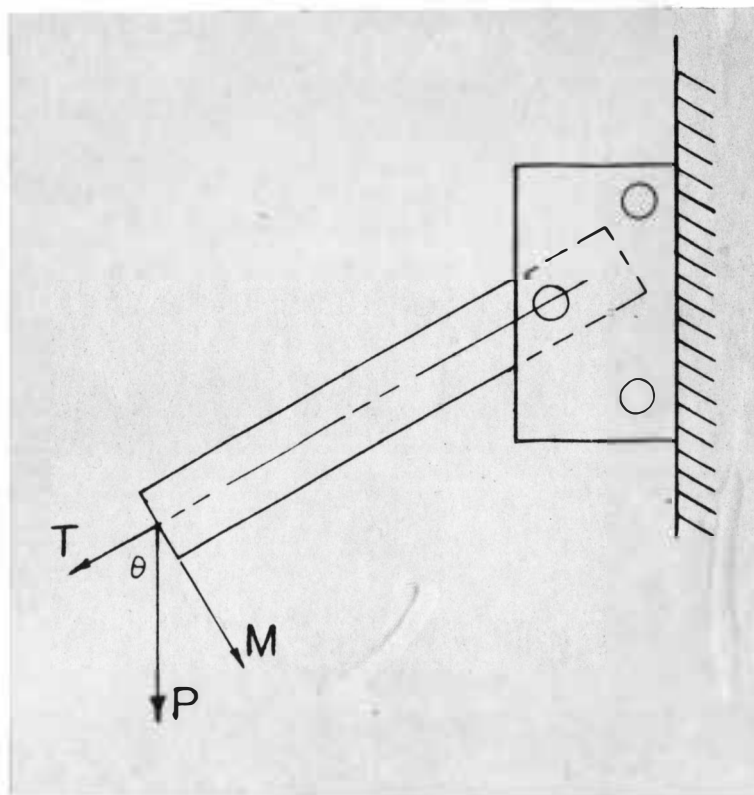


Figure XI. Ratio of Moment to Tension

D. Model Cutter

Plastic resins have the property of maintaining residual stresses when models are cut. Excessive heat and chipping will stress the material enough to alter the fringe pattern of a stressed model.

A high-speed precise cutting tool, Figure XII, planes the plastic resin. It eliminates the high heat and chipping effects. The unloaded velocity of the instrument is 45,000 rpm and tips of $\frac{1}{8}$ inch and $\frac{1}{4}$ inch are available for different cutting conditions.

Metal patterns are first machined of $\frac{1}{10}$ inch thick aluminum sheets. The plastic sheet is taped to the metal model with double-faced masking tape and is drawn along a guide below the cutting tip. There are two guides for each cutting tip, one for rough cutting and one for finish cutting.

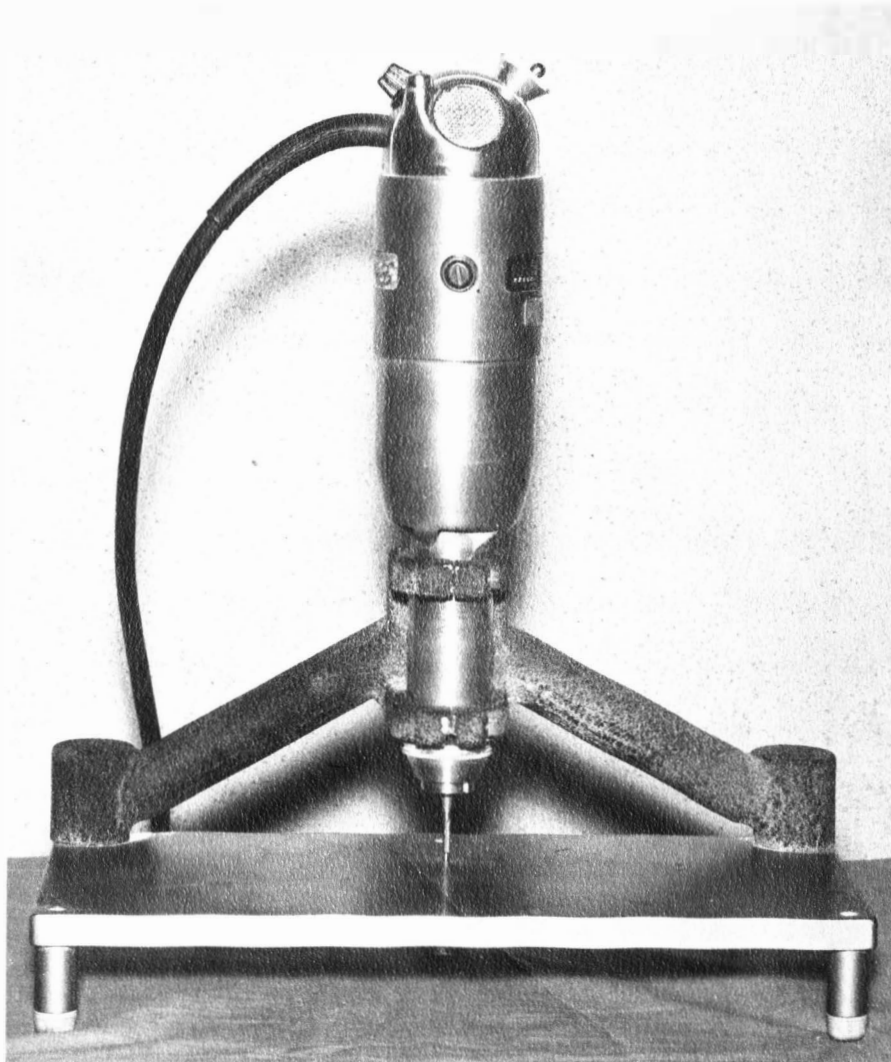


Figure XII. Precise Photoelastic Model Cutter.

CHAPTER IV

LABORATORY TEST PROCEDURE

A. Photoelastic Material and Equipment Arrangement

Model materials are selected on the basis of sensitiveness, ease of working and other mechanical properties.^{15/} A pattern is made to give the model proper dimensions as well as a smooth finish. The model can be easily checked for cutting stresses by removing the quarter-waveplates and observing the model in monochromatic light, Figure XIII and Figure XIV.

A complete stress picture is obtained from a combined usage of the isoclinic fringes and isochromatic lines. Isoclinic fringes are best observed by using a white light source with the plane polariscope. A light load is used to make the isoclinic fringes more discernable. Tracing the isoclinic fringes is a more precise method of recording than reading the fringes from a photograph. Monochromatic light is used to study isochromatic lines. Quarter-waveplates are used to extinguish the isoclinic fringes. By photographing the isochromatic fringes, greater detail can be obtained in regions of high stress concentration through picture enlargements.

^{15/} Filon, L. N. G., Photoelasticity for Engineers.
London: Cambridge University Press, 1936.

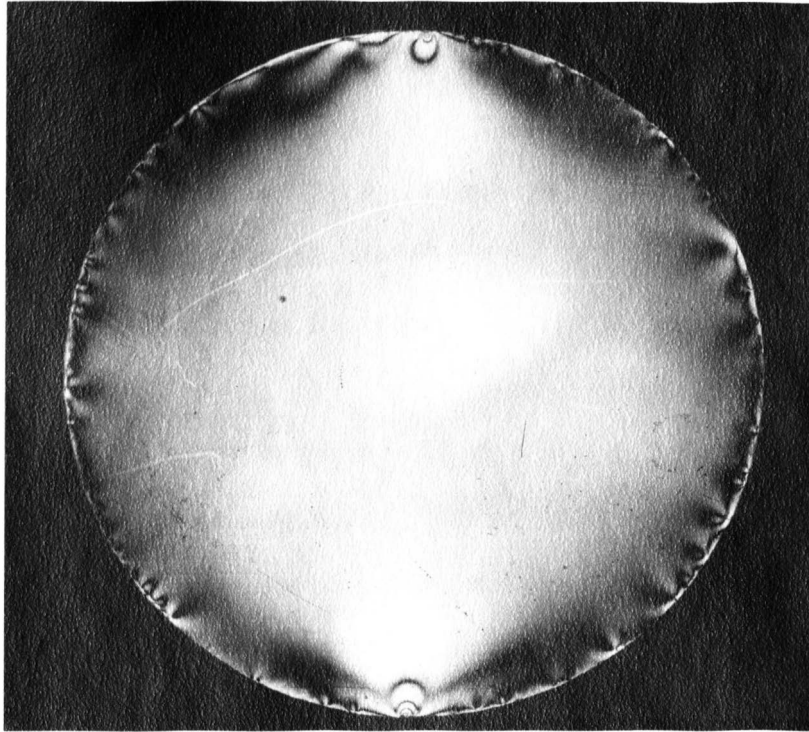


Figure XIII. Specimen before Annealing.

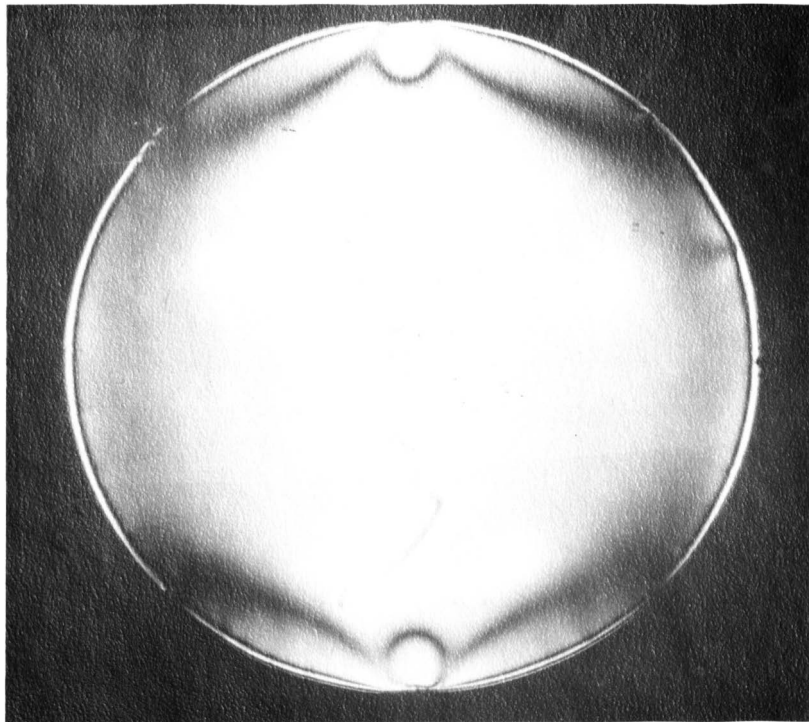


Figure XIV. Specimen after Annealing.

B. Fringe Calibration at Normal Temperature

Each piece of stock material should be tested to determine the stress-optic fringe constant. Three convenient test methods that exist are compression of a circular disk, a regular tension specimen, and a three stage specimen.

A three stage model is used because the fringes are clearly defined. The ratio of thicknesses of the stages is 6:4:3. According to the stress optic law, the number of fringes shown in Figure XV vary linearly according to Table 1 and the proportion $n_a = n_b = n_c = 6:4:3$.

Table 1. Fringe Ratio Under Varying Loads.

Picture	Load	n_a	n_b	n_c
1	0	0	0	0
2	22.0	1	$2/3$	$1/2$
3	42.6	2	$1 \frac{1}{3}$	1
4	59.1	3	2	$1 \frac{1}{2}$
5	77.0	4	$2 \frac{2}{3}$	2
6	94.9	5	$3 \frac{1}{3}$	$2 \frac{1}{2}$
7	113	6	4	3

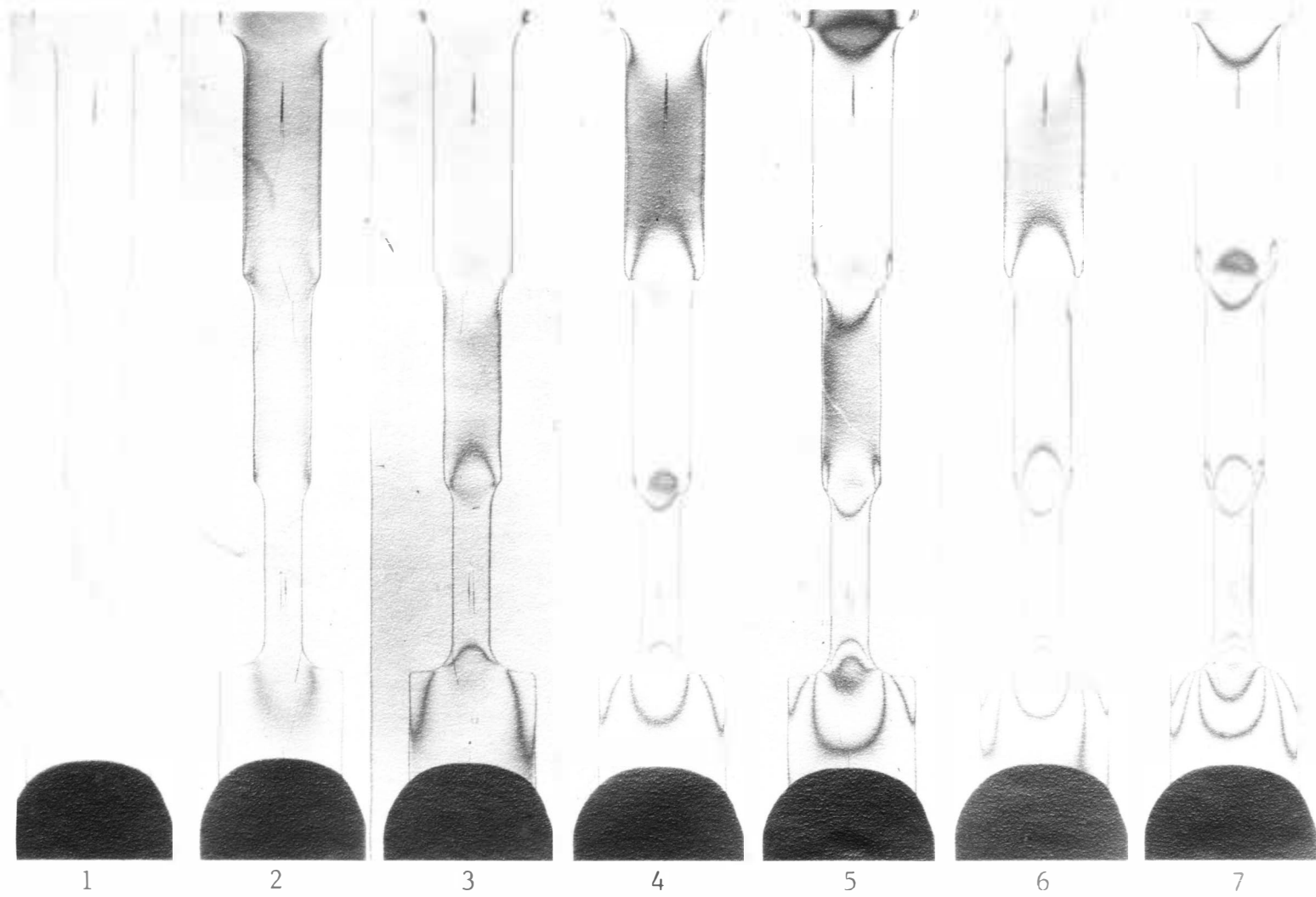


Figure XV. Sequential Photograph Showing
Linear Stress-Optic Relationship.

At the maximum load, 113 pounds, the specimen has the sixth fringe visible in the smallest section. From photoelastic methods, we see that

$$\sigma_1 - \sigma_2 = \frac{fn}{t} \quad \text{Eq. (16)}$$

By analytical methods principle stress difference in tension is

$$\sigma_1 - \sigma_2 = P/A, \quad \text{Eq. (17)}$$

therefore

$$\sigma_1 - \sigma_2 = \frac{fn}{t} = \frac{P}{td}$$

$$\frac{f (6 \text{ fringes})}{t} = \frac{113 \text{ lb}}{t (0.23 \text{ in})}$$

$$f = 82 \text{ lb/in/fringe.}$$

A standard tension specimen will give similar results.

For a load of 119.5 pounds, six fringes appear, Figure XVI. The fringe value for this specimen is

$$\sigma_1 - \sigma_2 = \frac{(n) f}{t} = \frac{P}{t (d)}$$

$$\frac{6 (f)}{t} = \frac{119.5 \text{ lb}}{t (0.24 \text{ in})}$$

$$f = 83 \text{ lb/in/f.}$$

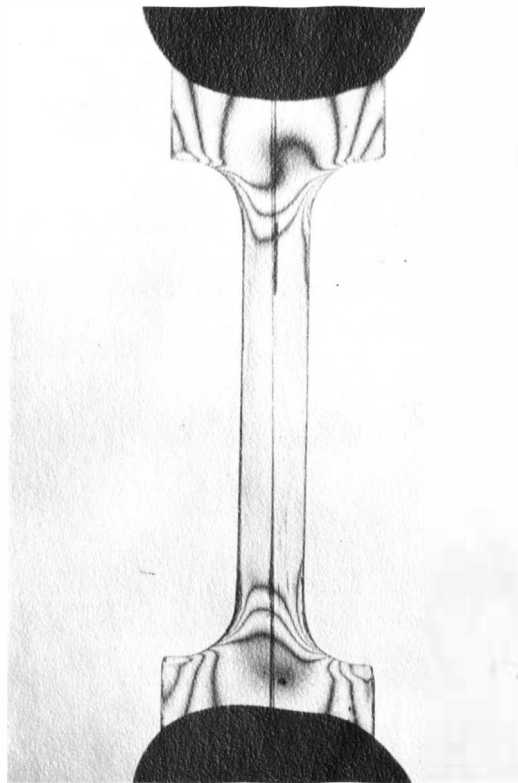


Figure XVI. Standard Tension Specimen.

The circular compression disk is used because the zero fringe is always visible, and the particular shape of the fringe pattern permits precise determination of the fringes at the center of the disk. The principal stress difference at the center of a circular disk by analytical methods^{16/} is

$$\sigma_1 - \sigma_2 = \frac{8 P}{tD\pi} \quad \text{Eq. (18)}$$

where

P = Diametrical load

t = Thickness of disk

D = Diameter of disk.

By photoelastic methods, the fringe value for the material shown in Figure XVII is

$$\sigma_1 - \sigma_2 = \frac{nf}{t} = \frac{8 P}{tD\pi}$$

$$\frac{(4.5) f}{t} = \frac{8 (369 \text{ lb})}{(t) (2.5 \text{ in})\pi}$$

$$f = 83.3 \text{ lb/in/fringe.}$$

^{16/} Timoshenko, S., and J. N. Goodier, Theory of Elasticity.
New York: McGraw Hill Book Company, Inc., 1951, pp. 107-108.

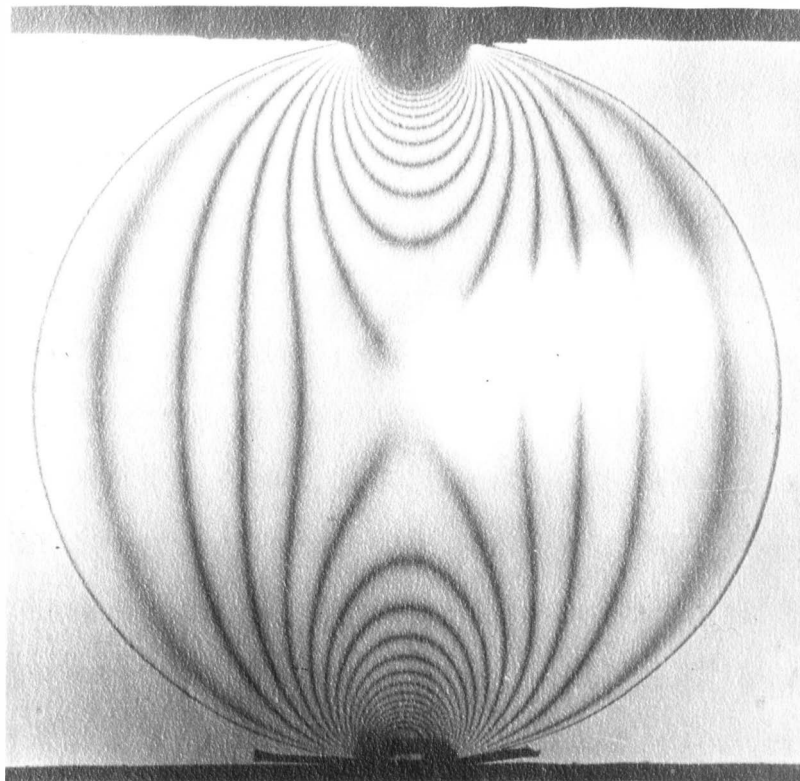


Figure XVII. Diametrically Loaded Circular Disk.

The average experimental fringe value obtained by the three test methods is 82.8 lb/in/fringe. This value compares favorably with the given^{17/} value of CR-39 which is 85 lb/in/fringe.

C. Fringe Calibration at Elevated Temperatures

Ordinary photoelastic studies are made on pieces which are loaded at room temperature. Because the material is elastic, the fringes will disappear when the load is removed.

Certain resins have the capability of holding the fringe patterns when they are loaded, heated and then cooled. It is explained^{18/} that these materials have a strong skeleton network which is unaffected by heat. The spaces are filled with a mass of loosely bonded molecules which soften on heating. When the model is cooled, the loose molecules "freeze" and cement the skeleton molecules to the position assumed when it is loaded. The optical effect is not disturbed by cutting the specimen for examination in a polariscope.

The fringe value of the material is changed greatly by the heating process. By the regular tension test specimen, the

^{17/}Hetenyi, p. 894.

^{18/}Timoshenko, p. 144.

fringe value is

$$\sigma_1 - \sigma_2 = \frac{f(n)}{t} = \frac{P}{td}$$

$$\frac{f(1.25 \text{ fringe})}{t} = \frac{5 \text{ lb}}{t(0.25 \text{ in})}$$

$$f = 16.0 \text{ lb/in/fringe.}$$

By the method of a compressed circular disk, Figure XVIII, the fringe value of stress-frozen CR-39 is

$$\sigma_1 - \sigma_2 = \frac{fn}{t} = \frac{8P}{td}$$

$$f = \frac{8(56.1 \text{ lb})}{(2.5 \text{ in})(3.6 \text{ f})}$$

$$f = 16.2 \text{ lb/in/f.}$$

Figure XIX shows that the fringes are undisturbed in a sliced model. An average value of 16.1 lb/in/fringe is obtained for stress-frozen CR-39 plastic resin.

Additional stresses are additive, but they add at the rate of fringe values for normal temperatures.

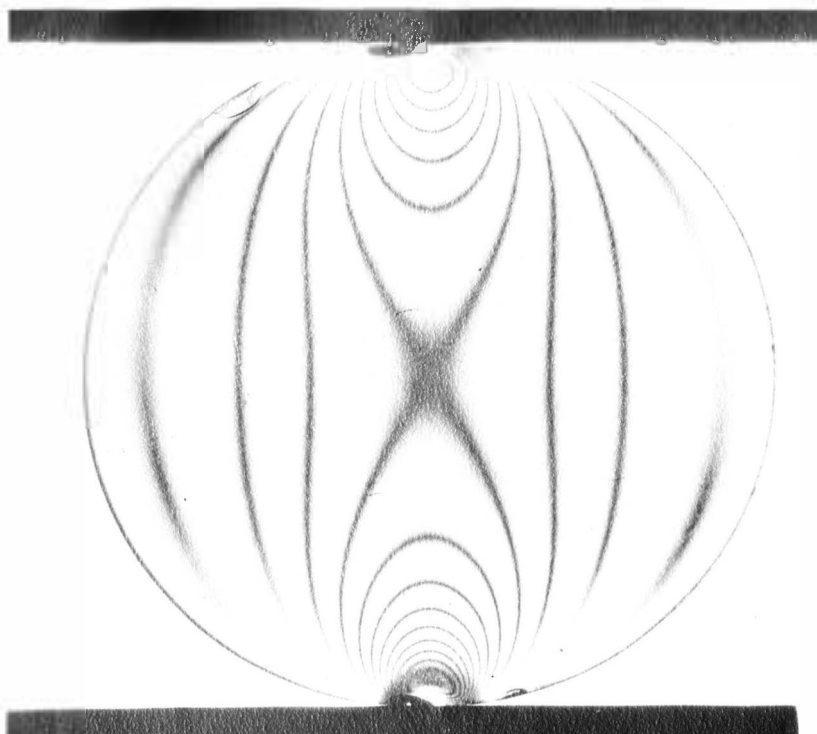


Figure XVIII. Frozen-Stress Pattern.

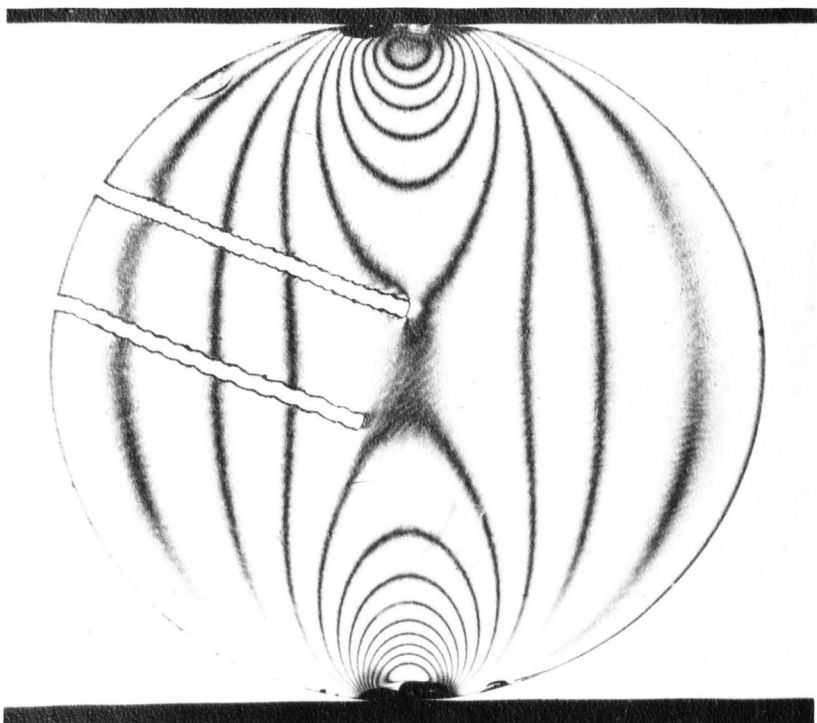


Figure XIX. Picture Showing Undisturbed Fringes in Frozen Model.

D. Determination of Stress Trajectories

Isoclinic lines themselves do not clearly describe the direction of the principal stresses. The directions of the principal stresses can be obtained from the plot of the stress-trajectories which are constructed from the isoclinic fringes.

The most successful method^{19/} of drawing these lines of principal stress is to construct the envelope of the curve. This envelope is constructed by drawing a series of tangents of intersection to the isoclinic lines so that they intersect at the midpoint between adjacent isoclinic fringes, Figure XX.

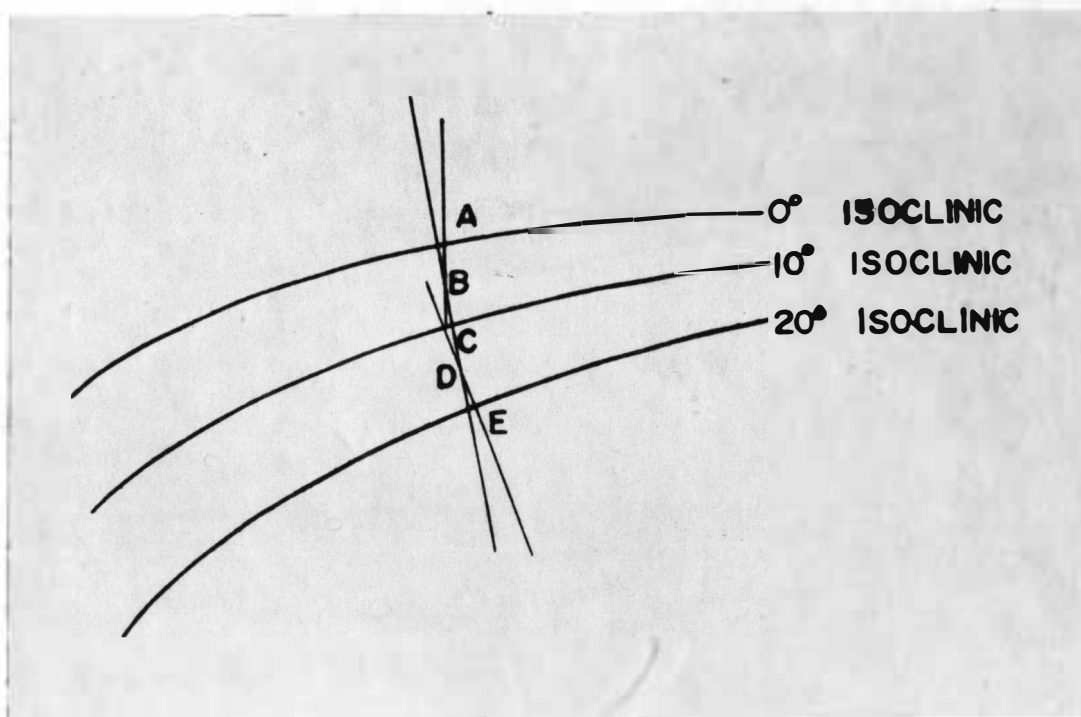


Figure XX. Construction of Lines of Principal Stress

^{19/} Jessop and Harris, p. 131.

Starting from some arbitrary reference point A, a 0° line is drawn through the 0° isoclinic. From the midpoint B, a second line is drawn at an inclination of 10° through the 10° isoclinic. After all of the isoclinics have been intersected, the line of principal stress is drawn with the french curve tangent to the constructed lines.

Some properties^{20/} of isoclinics which may be useful in determining stress trajectories are:

1. The isoclinic lines do not intersect one another (except at an isotropic point, Appendix B).
2. The isoclinic lines only intersect a free boundary where it has the inclination indicated for the isoclinic (except at a point of zero stress where all isoclinics may run into the free boundary).
3. A straight free boundary is also an isoclinic line.
4. All isoclinic lines intersect at an isotropic point. (At an isotropic point the two principal stresses are equal and are inclined in every conceivable direction.
5. An axis which is symmetrical with both the loads and geometry of the model coincides with one isoclinic.

CHAPTER V

CONCLUSIONS AND RECOMMENDATIONS

The tests performed show that the facilities available are adequate for either two- or three-dimensional photoelastic studies. Data can be obtained for a complete stress analysis or for a study of stress behavior under varying loading conditions.

Tests showed that the cooling rate of the stress-freezing oven can be slowed to 3 degrees per hour with 70 regular sized firebrick. Additional firebrick will retard the cooling rate further. Three problems exist in oven control:

1. The Variac is too coarse of precise control of small temperature differences. A smaller Variac should be connected either in series with the large Variac or directly to one of the four heating coils. This Variac would give a finer voltage control, and consequently closer temperature control.
2. At a temperature of 200 degrees Fahrenheit there is a gradient of 20 Fahrenheit degrees within the oven from top to bottom. Model temperature must be measured by placing a thermocouple next to the specimen.
3. The line voltage varies at different times during a day. Although the insulation of the oven is sufficient

to cancel most of the effects of the voltage change, extremely precise temperature control would require the use of an automatic voltage regulator.

Generalized loading frames have been designed for loading models in the stress-freezing oven. Regular shaped models can be loaded on the available loading frames, but additional attaching fixtures may be necessary for special loading problems. A universal loading frame would be impossible to design because of the infinite number of applications of photoelastic methods.

BIBLIOGRAPHY

1. Coker, E. G. and L. N. G. Filon, A Treatise on Photoelasticity. London: Cambridge University Press, 1931.
2. Dove, Richard C., and Paul H. Adams, Experimental Stress Analysis and Motion Measurement. Columbus: Charles E. Merrill Books, Inc., 1964.
3. Filon, L. N. G., Photoelasticity for Engineers. London: Cambridge University Press, 1936.
4. Frocht, M. M., Photoelasticity, Vols. 1 and 2. New York: John Wiley and Sons, 1941, 1948.
5. Hetenyi, M., Handbook of Experimental Stress Analysis. New York: John Wiley and Sons, Inc., 1950.
6. Higdon, A., E. H. Ohlsen and W. B. Stiles, Mechanics of Materials. New York: John Wiley and Sons, Inc., 1960.
7. Jessop, H. T. and F. C. Harris, Photoelasticity Principles and Methods. New York: Dover Publications, Inc., 1949.
8. Richards, J. A., Sears, F. W., Wehr, M. R. and Zemansky, M. W., Modern University Physics. Reading, Mass.: Addison-Wesley Publishing Company, Inc., 1960.
9. Timoshenko, S., and J. N. Goodier, Theory of Elasticity. New York: McGraw Hill Book Company, Inc., 1951.

APPENDIX A

CALCULATION OF STRESSES ALONG A LINE OF PRINCIPAL STRESS
IN A COMPRESSED CIRCULAR DISK

The stress-trajectory DC in Figure XXII cuts the isoclinic lines at angles varying from 50 degrees to 90 degrees. Filon's form of the Lamé-Maxwell equations,^{21/} Eq. (15) for equilibrium fits the given conditions.

$$P = (P - Q) \cot \psi \cdot \delta \phi \quad \text{Eq. (15)}$$

The quantities included are

- δP = increment of P along the p line of principal stress
- $P - Q$ = principal stress difference to be taken from Figure XXIII
- ϕ = isoclinic parameter
- ψ = angle between p line and the isoclinic

The values of principal stresses (P - Q) are taken from a plot of the principal stresses along the line of interest, Figure XXIII. A tabular form is set up for points C-D on the disk.

^{21/} Jessop, H. T. and F. C. Harris, p. 18.

TABLE 2.
Tabular Form for P and Q Values on Circular Disk.

1	2	3	4	5	6	7	8	9	10	11
Point	(P - Q)	P - Q	ψ	$\cot \psi$	(P - Q)	(P - Q)	$\delta \phi$	δP	P	Q
	Rel Ret	lb/sq in	Degrees		lb/sq in	(mean)	rad	lb/sq in	lb/sq in	lb/sq in
	δ									
D	0	0	50	0.84	0	80.5	0.175	14.1	0	0
E	0.55	199	51	0.81	161	270.5	0.175	47.5	14	-185
F	1.4	507	53	0.75	380	496.0	0.175	86.8	62	-445
G	2.6	942	57	0.65	612	661.0	0.175	115.8	148	-794
H	4.0	1450	64	0.49	710	660.0	0.175	115.5	264	-1186
J	5.2	1880	72	0.33	610	305.0	0.175	53.4	380	-1500
C	5.7	2060	90	0.0	0				433	-1627

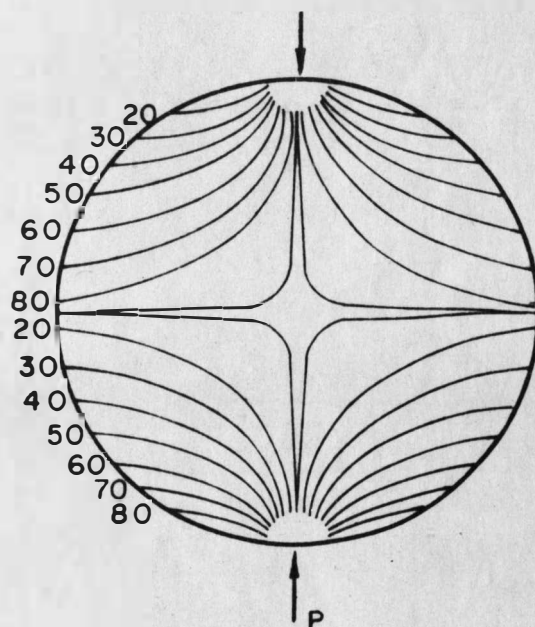


Figure XXI. Isoclinic Fringes in Compressed Disk.

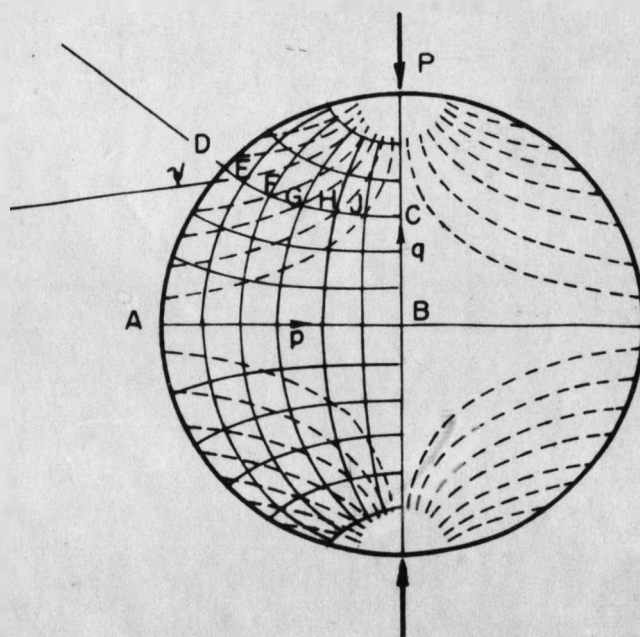


Figure XXII. Stress Trajectories in Compressed Disk.

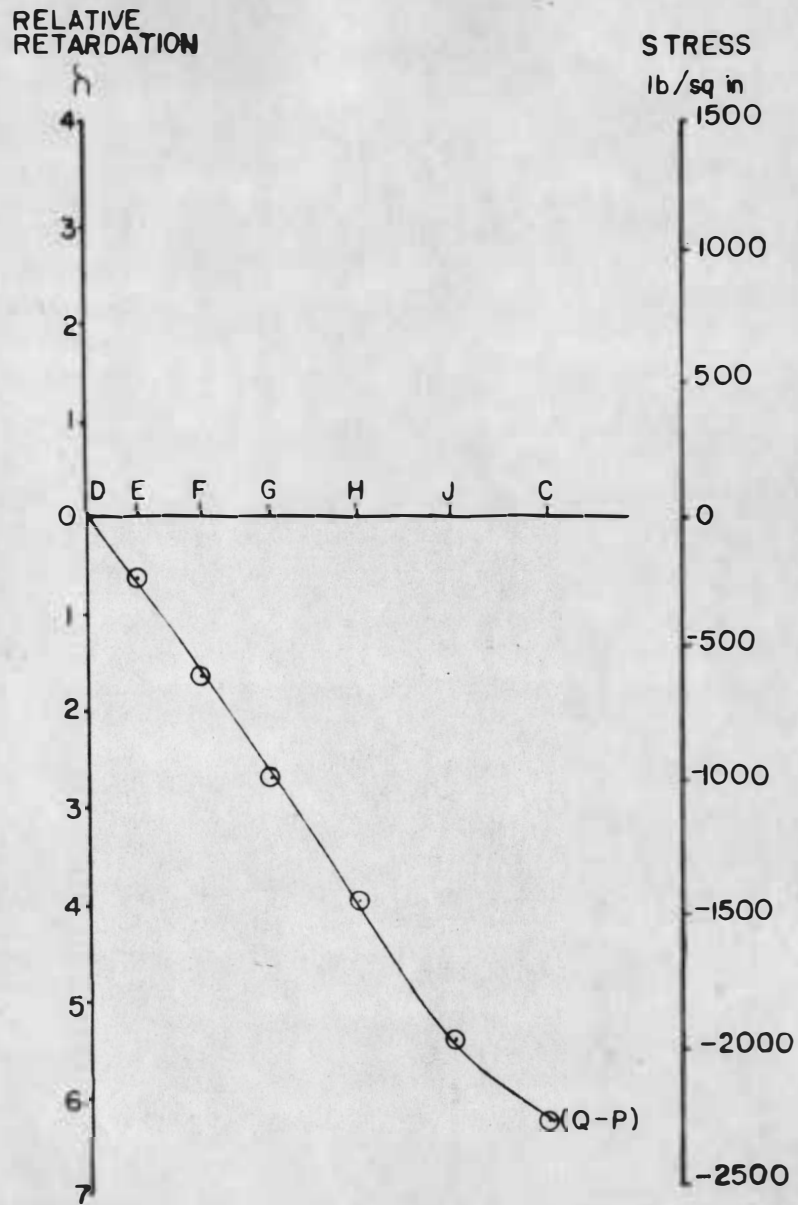


Figure XXIII. Relative Retardation in Compressed Disk Shown in Figure XVII.

APPENDIX B

ISOTROPIC POINT IN A CURVED BEAM

Isotropic points are a valuable tool in the interpretation of stresses in a photoelastic specimen. The principal stress difference is zero or $P = Q$ at an isotropic point, consequently, the isochromatic fringes can be counted using this point as a reference.

Two interesting characteristics occur when viewing isotropic points. The isochromatic fringes form a hole or ellipse from which fringes appear to originate. Isoclinic fringes can join or cross only at an isotropic point, Figure XXIV and Figure XXV.

Isostatic lines or stress trajectories form loops around an isotropic point but never actually intersect it, Figure XXVI.

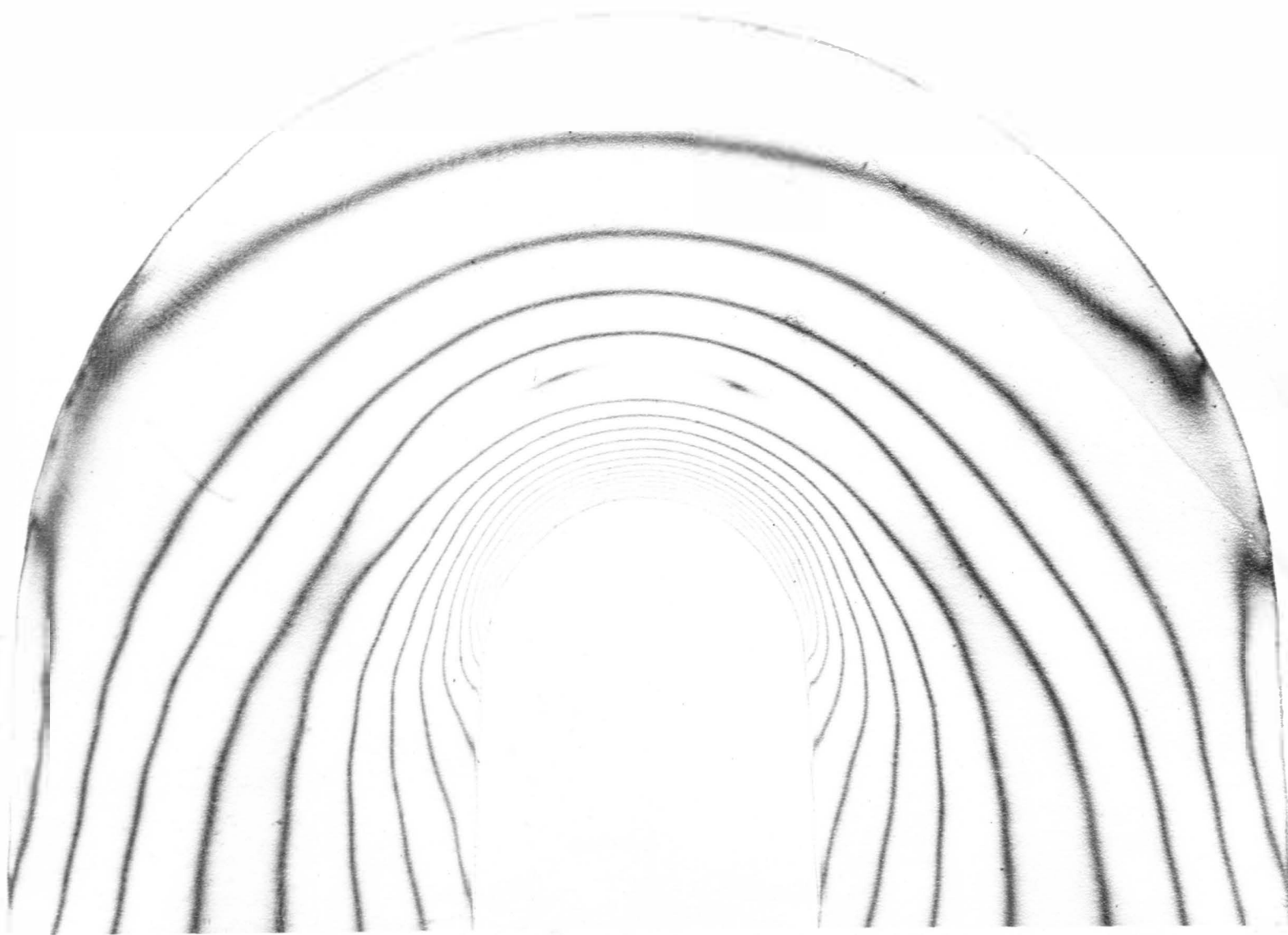


Figure XXIV. Curved Beam Specimen.

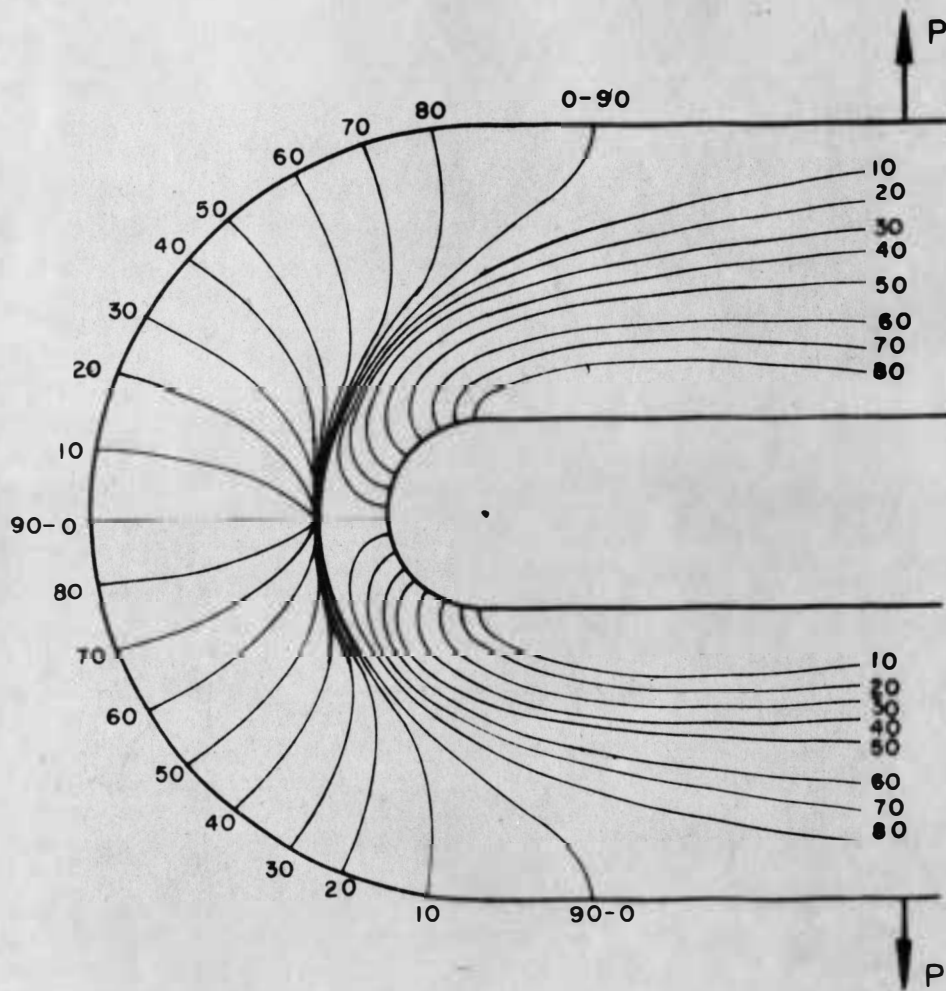


Figure XXV. Isoclinics in Curved Beam Specimen.

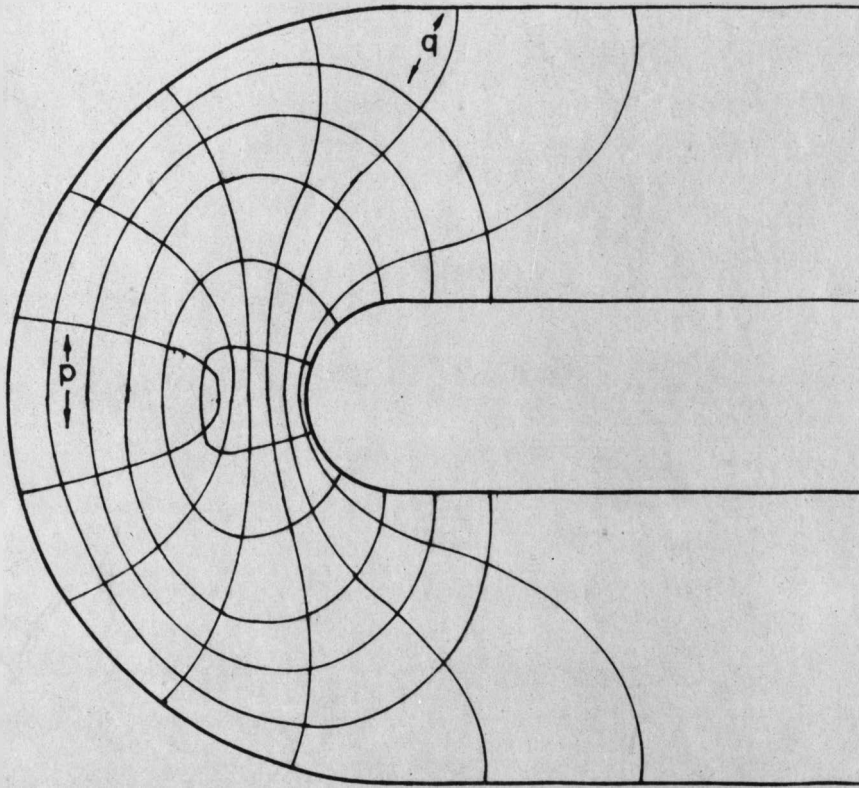


Figure XXVI. Sketch of Stress Trajectories in a Curved Beam.

APPENDIX C**COOLING CURVES FOR STRESS-FREEZING OVEN**

Voltage for 185°F critical temperature = 50.5 volts

Soaking time for CR-39 = 6 hours

Lined oven = 70 standard firebrick

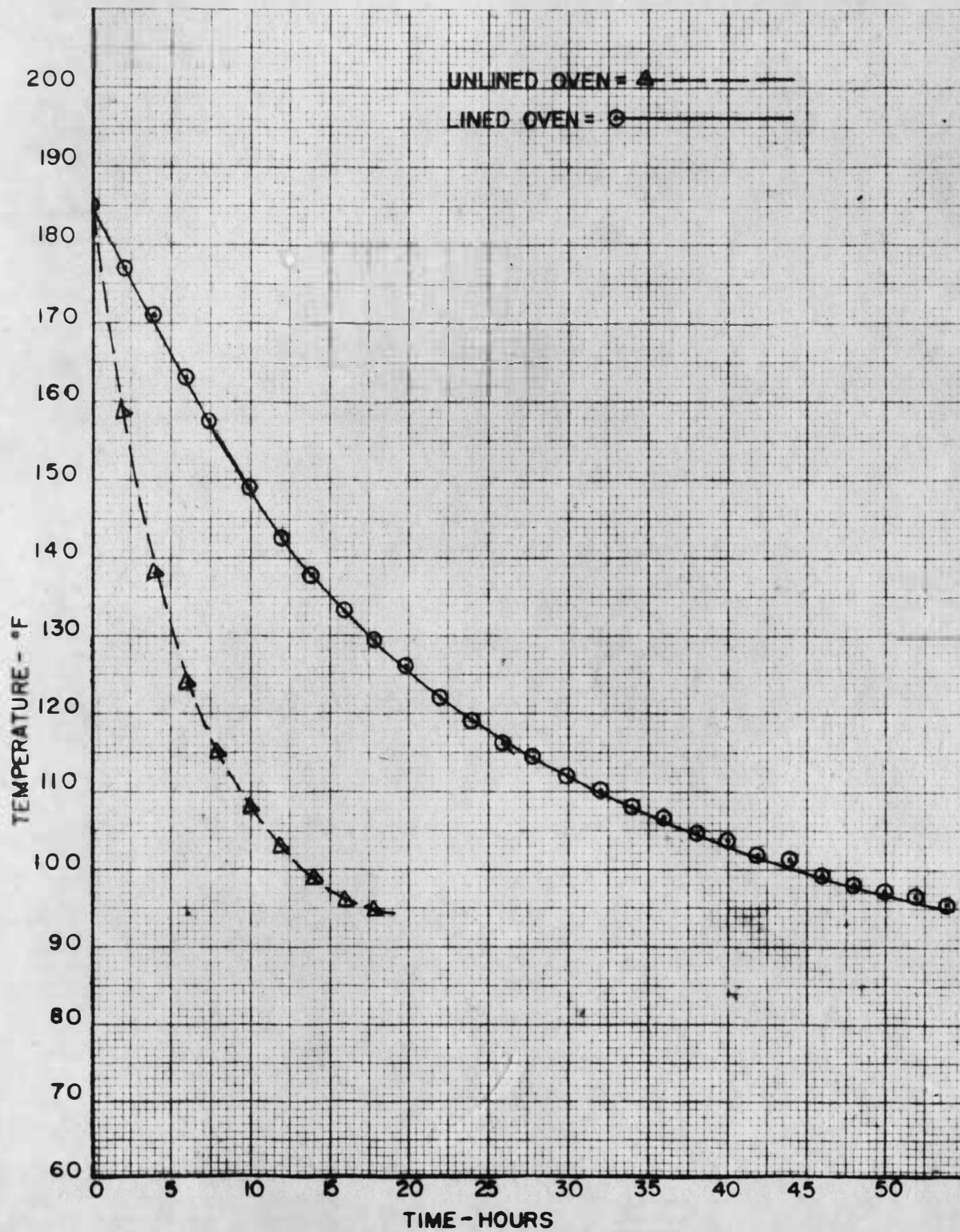


FIGURE XXVII COOLING CURVES FOR STRESS-FREEZING OVEN

APPENDIX D

SYMBOLS USED

- e = a constant
 t = time
 x = a variable distance along the X-axis
 y = a variable distance along the Y-axis
 ϕ = any angle
 θ_p = the angle between the principal plane and some reference plane
 σ_x = normal stress at a point in the X-direction
 σ_1 = maximum principal stress
 σ_y = normal stress at a point in the Y-direction
 σ_2 = minimum principal stress
 τ_{xy} = a shear couple at a point